

# Structural Determinants for Potent, Selective Dual Site Inhibition of Human pp60<sup>c-src</sup> by 4-Anilinoquinazolines

Gaochao Tian,<sup>\*,‡,§</sup> Michael Cory,<sup>||</sup> Albert A. Smith,<sup>‡</sup> and W. Blaine Knight<sup>‡</sup>

Departments of Molecular Biochemistry and Structural Chemistry, GlaxoSmithKline Research and Development, Research Triangle Park, North Carolina 27709

Received January 9, 2001; Revised Manuscript Received April 27, 2001

**ABSTRACT:** The kinetic mechanisms for the inhibition of pp60<sup>c-src</sup> tyrosine kinase (Src TK) by 4-anilinoquinazolines, an important class of chemicals as protein kinase inhibitors, were investigated. 4-Anilinoquinazolines with a bulky group at the 4'-position of the anilino group were shown to be competitive with both ATP and peptide, whereas molecules lacking such a bulky group only displayed an inhibition pattern typical of those competitive with ATP and noncompetitive with peptide. Modifications of the substituents on the carbocyclic ring did not perturb the inhibition pattern although the affinities of these modified inhibitors for Src TK were affected. Structural modeling of Src TK with inhibitor and peptide substrate bound indicated a direct atomic conflict between the bulky 4-position group and the hydroxy of the peptide tyrosyl to which the  $\gamma$ -phosphate of ATP is transferred during the kinase reaction. This atomic conflict would likely prevent simultaneous binding of both inhibitor and peptide, consistent with the observed kinetic competitiveness of the inhibitor with peptide. The dual site inhibitors appeared to have both enhanced potency and selectivity for Src TK. One such inhibitor, 4-(4'-phenoxyanilino)-6,7-dimethoxyquinazoline, had a 15 nM potency against Src TK and was selective over receptor tyrosine kinases VEGFR2 by 88-fold and C-fms by 190-fold.

Protein kinases are crucial components of the signal transduction pathways that are central to cellular and biological functions (1, 2). Consequently, enhanced activities of protein kinases have been linked to many diseases such as cancer, diabetes, and inflammatory conditions (3–6). Inhibition of protein kinases is currently a popular approach taken by the pharmaceutical industry for developing effective treatments of these diseases (7–15). These drug discovery efforts have led to increased understanding of the kinetics, mechanisms, structures, and interactions of small molecule inhibitors of protein kinases, thus providing a framework for rational design of protein kinase inhibitors.

Given that protein kinases have two substrate-binding sites, three mechanisms could be exploited to inhibit a protein kinase: targeting (a) the ATP<sup>1</sup>-binding site, (b) the peptide-binding site, or (c) both the ATP and peptide sites simultaneously. Since ATP is a substrate shared among all protein kinases and the ATP-binding site of protein kinases is relatively conserved (16, 17), selectivity could be an issue

in targeting this site alone. Although recent data suggest that the conformational structure of the ATP site is quite diverse among protein kinases and, in certain cases, inhibitors of homologous protein kinases can be very selective (7, 11, 14, 15, 18, 19), developing ATP site inhibitors with high selectivity remains a challenging task. The peptide-binding site provides a potentially good alternative target for developing selective inhibitors given that the peptide site shows lower homology than the ATP site shared between protein kinases. However, the peptide site is generally shallow and largely exposed to solvent, and, therefore, it is difficult to develop inhibitors with sufficiently high potency and to meet *in vivo* efficacy requirements. It is conceivable that a dual site inhibitor could be potent and, yet, provide a selectivity advantage. Most of the inhibitors of protein kinases identified so far are competitive with ATP, few are specific for the peptide site, and only a handful of dual site inhibitors are known to date (9, 20–22). For those known dual site inhibitors, the mechanism of action and the structural features responsible for the observed dual site inhibition are poorly understood.

In the current study, we investigated the kinetics of inhibition of pp60<sup>c-src</sup> tyrosine kinase (Src TK) by 4-anilinoquinazolines, a class of compounds that have been reported to inhibit a number of protein kinases, such as EGFR TK (23), CDK2 (24), and p38 kinase (24). Similar to many other protein kinase inhibitors, many 4-anilinoquinazolines displayed a typical inhibition pattern that is competitive with ATP and noncompetitive with peptide. To our surprise, relatively small changes in substituents at the anilino group of 4-anilinoquinazolines caused the compounds to become

\* To whom correspondence should be addressed (Tel: 302-886-8137; Fax: 302-886-4983; Email: gaochao.tian@astrazeneca.com).

<sup>‡</sup> Department of Molecular Biochemistry.

<sup>§</sup> Current address: Department of Lead Discovery, AstraZeneca Pharmaceuticals, 1800 Concord Pike, PO Box 15437, Wilmington, DE 19850-5437.

<sup>||</sup> Department of Structural Chemistry.

<sup>1</sup> Abbreviations: ATP, adenosine 5'-triphosphate; BSA, bovine serum albumin; CDK2, cyclin-dependent kinase 2; DMSO, dimethyl sulfoxide; EGFR, epidermal growth factor receptor; IR, insulin receptor; HEPES, *N*-(2-hydroxyethyl)piperazine-*N'*-2-ethanesulfonic acid; LDH, lactate dehydrogenase; NADH, reduced nicotinamide adenine dinucleotide; PEP, phosphoenolpyruvate; PK, pyruvate kinase; Src, pp60<sup>c-src</sup>; TK, tyrosine kinase; VEGFR, vascular endothelial growth factor receptor.

dual site inhibitors that are competitive with both ATP and peptide and resulted in increased potency as well as enhanced selectivity. Computer modeling according to reported Src TK structures and binding modes of known 4-anilinoquinazoline-kinase cocrystals was performed in order to understand the structural and mechanistic changes. The results from the computer modeling supported the dual site inhibition as suggested by the kinetic data and provided a structural model upon which further improvements in potency and selectivity of 4-anilinoquinazolines for Src TK may be designed.

## EXPERIMENTAL PROCEDURES

**Materials.** The peptide substrate for Src tyrosine kinase, acetyl-EEIYGEI-NH<sub>2</sub>, was purchased from Synpep. ATP, MgCl<sub>2</sub>, BSA, HEPES, PEP, PK, LDH, and pyruvate were of reagent grade from Sigma. Stock solutions of peptide, ATP, MgCl<sub>2</sub>, and NADH were prepared in 100 mM HEPES, pH 7.5. Stock solutions of PEP and pyruvate were prepared in 100 mM HEPES, and the final pH was adjusted to 7.5 with NaOH. PK and LDH stocks were prepared in H<sub>2</sub>O and then mixed with the stock solutions of PEP, NADH, and pyruvate to form a single stock solution. This single stock was then aliquoted and stored at -80 °C prior to use.

**Preparation of Quinazolines.** 4-Anilinoquinazolines were prepared from coupling the corresponding 4-chlorodimethoxyquinazoline and aniline according to literature procedures (25).

**Construction, Expression, and Purification of Src TK.** A recombinant Src TK (dm-Src TK) was expressed in baculovirus as an N-85 protein deletion mutant with two point mutations, Y338F and Y530F, and purified according to Ellis et al. (26).

**Spectrophotometric Assays of dm-Src TK.** Prior to performing an assay, dm-Src TK was preactivated by incubating enzyme (~30 μM) with 10 mM MgCl<sub>2</sub> and 1 mM ATP in 100 mM HEPES, pH 7.5, containing 0.1 mg/mL BSA at 4 °C for 40 min to allow for enzyme autophosphorylation (27). The spectrophotometric assay of dm-Src TK was performed according to Edison et al. (28) with minor modifications. The phosphorylation of peptide and the production of ADP were coupled to the oxidation of NADH using PEP, PK, and LDH and monitored by following the decrease in absorbance at 340 nm (*A*<sub>340</sub>). Then 200 μL reaction mixtures were prepared in a clear flat-bottom 96-well plate (Costar) and contained 1 mM PEP, 0.3 mM NADH, 25 units/mL PK, 60 units/mL LDH, 0.1 mg/mL BSA, 5% DMSO with or without inhibitor, varying concentrations of ATP and peptide, and activated dm-Src TK at a concentration in the range of 4–50 nM. The reactions were initiated by addition of enzyme. *A*<sub>340</sub> values of progress curves were recorded by a 96-well plate reader (SpectraMax 250, Molecular Device) at room temperature (22 °C).

**Data Analysis.** Initial rates (mOD/min) were determined by a linear least-squares regression analysis of the progress curves obtained from spectrophotometric measurements as described above. The initial rates in mOD/min were then converted to values in μM/min using the extinction coefficient of 3.41 mOD/mM for NADH in 200 μL reaction solutions in 96-well plates with a path length of 0.55 cm.

The initial rates as a function of both substrate concentrations were fitted to eq 1 (29) for a fast equilibrium random mechanism as it was described previously for Src TK (30):

$$v = \frac{VAB}{K_{ia}K_b + K_aB + K_bA + AB} \quad (1)$$

where *v* is the measured initial rate, *V* is the maximum velocity, *A* and *B* are the concentrations for substrates A and B, respectively, *K*<sub>ia</sub> is the dissociation constant for the binary EA complex, and *K*<sub>a</sub> and *K*<sub>b</sub> are the Michaelis–Menten constants for A and B, respectively. For inhibitors which are competitive vs A and noncompetitive vs B, the inhibition data from variation of A and B, respectively, were fitted to (29)

$$v = \frac{V_b A}{(K_a)_b \left(1 + \frac{I}{K_{is}}\right) + A} \quad (2)$$

and

$$v = \frac{V_a B}{(K_b)_a \left(1 + \frac{I}{K_{is}}\right) + B \left(1 + \frac{I}{K_{ii}}\right)} \quad (3)$$

where *V*<sub>b</sub> and (*K*<sub>a</sub>)<sub>b</sub> are, respectively, the apparent maximum velocity at a fixed *B* and the Michaelis–Menten constants for A at a fixed *B*; *V*<sub>a</sub> and (*K*<sub>b</sub>)<sub>a</sub> are, respectively, the apparent maximum velocity at a fixed *A* and the Michaelis–Menten constants for B at a fixed *A*; *I* is the concentration of inhibitor I; and *K*<sub>is</sub> and *K*<sub>ii</sub> are, respectively, the slope and intercept inhibition constants. Equation 2 was also used for fitting data obtained for dual site inhibitors, which are competitive vs both substrates. For dual site inhibitors, the inhibition constant for the binary EI complex, *K*<sub>i</sub>, was calculated by using eq 4 (eq A7, Appendix):

$$K_i = \frac{K_{is}}{1 + \frac{B}{K_{ib}}} \quad (4)$$

where *K*<sub>ib</sub> is the dissociation constant for the binary complex EB. For inhibitors competitive vs A and noncompetitive vs B, from variation of A, *K*<sub>i</sub> was calculated by using eq 5 (31):

$$K_i = K_{is} \frac{1 + \frac{B/\beta}{K_b}}{1 + \frac{B}{K_{ib}}} \quad (5)$$

where

$$\beta = \frac{K'_i}{K_i} \quad (6)$$

in which *K*'<sub>i</sub> is the inhibition constant for the ternary complex EBI. From variation of *B*, *K*<sub>i</sub> was calculated by using (31)

$$K_i = \frac{K_{is}}{1 + \frac{A}{K_{ia}}} \quad (7)$$

and  $K_i'$  was calculated by using (31)

$$K_i' = \frac{K_{ii}}{1 + \frac{A}{K_a}} \quad (8)$$

**Computer-Graphic Modeling.** Src protein and ligand complex computer models were generated from protein databank structures and energy-minimized models of the ligands (32). The molecular modeling program MacroModel (Version 7) was used for the superposition of protein structures and subsequent molecular mechanics modeling. The all-atom Amber force field as implemented in MacroModel was used for the molecular mechanics computations (33). Only one tyrosine kinase structure is available with a substrate, or substrate model, bound to the protein. This structure is the insulin receptor tyrosine kinase (protein databank file 1ir3.pdb) (34) with an 18 amino acid peptide substrate. This structure was used as the starting point for the substrate sequence modeled into Src. As an initial starting point, for Src, the crystal structure 2src.pdb (35) was used. Into this structure was docked the  $\alpha$ -helical structure of the substrate sequence acetyl-AAEEIYGEI-NH<sub>2</sub>, which is the substrate sequence used in the enzyme assays. Initial starting points for the model were obtained by superposition of insulin receptor kinase over the Src TK, with the superposition atoms being those of the ATP group. Different conformations for the phosphate groups of ATP were found in the two structures, and, thus, only the adenine and the ribose atoms were used in the superposition.

Compounds **1**, **4**, and **9** were docked into the Src model containing the substrate. The starting point for these ligands was the conformation seen in CDK2 and p38 for similar compounds (24). Conformational searches of the flexible bonds of the ligands were done keeping the protein rigid with force field constraints. After the conformational search, additional minimizations allowing movement of the protein were done, with the found ligand conformations.

## RESULTS AND DISCUSSION

**Kinetic Properties of dm-Src TK.** The Src TK used in this study was a variant of N-85, a truncated mutant of Src TK (30), which will be hereby referred to as “wt-Src TK”. This variant of N-85 had two point mutations (Y338F; Y530F) and will be hereby referred to as “dm-Src TK”. This double mutant was designed for producing a more homogeneous protein preparation (26). The kinetic mechanism of wt-Src TK was determined previously to be a sequential bi-bi rapid equilibrium random mechanism (30). The kinetic pattern (Figure 1) of dm-Src TK, as probed by varying both [ATP] and [peptide], was similar to the pattern reported for wt-Src TK (30). The kinetic properties of dm-Src TK, as determined by fitting the kinetic data to eq 1, were also similar to the kinetic properties obtained previously for wt-Src TK (Table 1). The mode of inhibition of dm-Src TK probed by using dead end inhibitors was also consistent with a bi-bi rapid equilibrium random mechanism (data not shown) as it was reported for the wild type (30). Kinetic data subsequently obtained for dm-Src TK were then treated assuming that dm-Src TK followed a bi-bi rapid equilibrium random mechanism.

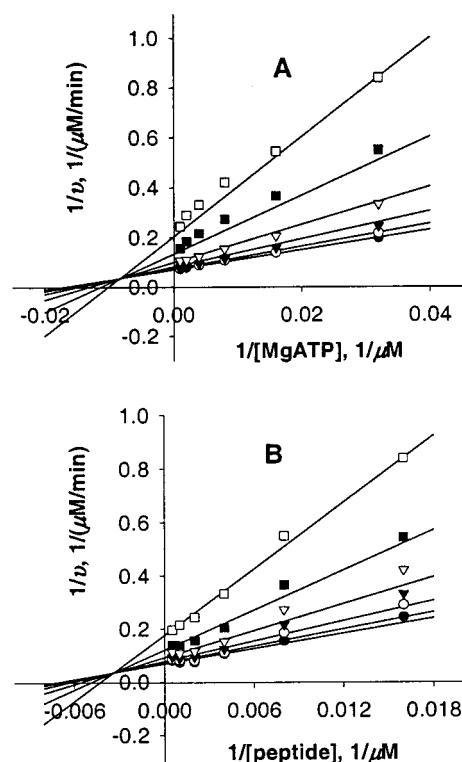
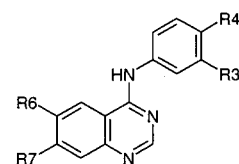


FIGURE 1: Kinetics of dm-Src TK. (A) Double-reciprocal plot of  $1/v$  vs  $1/[MgATP]$  ( $[MgATP]$  = 1000, 500, 250, 125, 62.5, and 31.25  $\mu$ M) at  $[peptide]$  = 62.5 ( $\square$ ), 125 ( $\blacksquare$ ), 250 ( $\nabla$ ), 500 ( $\blacktriangledown$ ), 1000 ( $\circ$ ), and 2000 ( $\bullet$ )  $\mu$ M. (B) Double-reciprocal plot of  $1/v$  vs  $1/[peptide]$  ( $[peptide]$  = 2000, 1000, 500, 250, 125, and 62.5  $\mu$ M) at  $[MgATP]$  = 31.25 ( $\square$ ), 62.5 ( $\blacksquare$ ), 125 ( $\nabla$ ), 250 ( $\blacktriangledown$ ), 500 ( $\circ$ ), and 1000 ( $\bullet$ )  $\mu$ M.

Table 1: Kinetic Properties of Src TK Constructs at pH 7.5, 22 °C

enzyme	$k_{cat}$ , s <sup>-1</sup>	$K_a$ , $\mu$ M	$K_b$ , $\mu$ M	$K_{ia}$ , $\mu$ M	$K_{ib}$ , $\mu$ M
wt-Src TK <sup>a</sup>	3100 $\pm$ 140	80 $\pm$ 11	82 $\pm$ 8	200	190
dm-Src TK <sup>b</sup>	2200 $\pm$ 99	55 $\pm$ 10	134 $\pm$ 24	120	294

<sup>a</sup> From Boerner et al. (30). <sup>b</sup> The kinetic parameters were obtained from nonlinear least-squares analysis of data according to eq 1.



- 1: R6 = OCH<sub>3</sub>; R7 = OCH<sub>3</sub>; R3 = Cl; R4 = Cl
- 2: R6 = OCH<sub>3</sub>; R7 = OCH<sub>3</sub>; R3 = OH; R4 = H
- 3: R6 = OCH<sub>3</sub>; R7 = OCH<sub>3</sub>; R3 = OCH<sub>3</sub>; R4 = H
- 4: R6 = OCH<sub>3</sub>; R7 = OCH<sub>3</sub>; R3 = H; R4 = OC<sub>6</sub>H<sub>5</sub>
- 5: R6 = OCH<sub>3</sub>; R7 = OCH<sub>3</sub>; R3 = H; R4 = NHC<sub>6</sub>H<sub>5</sub>
- 6: R6 = H; R7 = NH<sub>2</sub>; R3 = H; R4 = OC<sub>6</sub>H<sub>5</sub>
- 7: R6 = H; R7 = H; R3 = H; R4 = OC<sub>6</sub>H<sub>5</sub>
- 8: R6 = OCH<sub>3</sub>; R7 = OCH<sub>3</sub>; R3 = H; R4 = OCH<sub>2</sub>C<sub>6</sub>H<sub>5</sub>
- 9: R6 = OCH<sub>3</sub>; R7 = OCH<sub>3</sub>; R3 = H; R4 = OCH<sub>2</sub>CH<sub>2</sub>OC<sub>6</sub>H<sub>5</sub>
- 10: R6 = OCH<sub>3</sub>; R7 = OCH<sub>3</sub>; R3, R4 = -CH=CHNH-

FIGURE 2: Chemical structures of 4-anilinoquinazolines for which kinetic inhibition mechanisms were investigated in this study.

**Kinetic Inhibition of dm-Src TK.** The structures of 4-anilinoquinazolines for which kinetic inhibition mechanisms were investigated in this study are given in Figure 2. The kinetic inhibition patterns for three 4-anilinoquinazolines, **1** (Figure 3), **2** (data not shown), and **3** (data not shown), were competitive with ATP and noncompetitive with peptide,

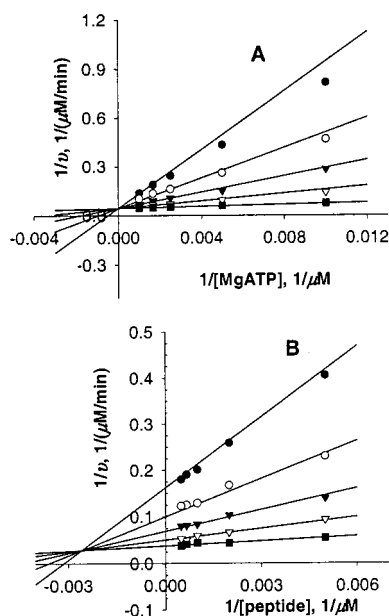


FIGURE 3: Inhibition of the dm-Src TK reaction by **1**. (A) Double-reciprocal plot of  $1/v$  vs  $1/[\text{MgATP}]$  ( $[\text{MgATP}] = 1000, 600, 400, 200$ , and  $100 \mu\text{M}$ ) at  $[I] = 0$  (■),  $0.4$  (▽),  $1$  (▼),  $2$  (○), and  $4$  (●)  $\mu\text{M}$ . (B) Double-reciprocal plot of  $1/v$  vs  $1/[\text{peptide}]$  ( $[\text{peptide}] = 2000, 1500, 1000, 500$ , and  $200 \mu\text{M}$ ) at  $[I] = 0$  (■),  $0.4$  (▽),  $1$  (▼),  $2$  (○), and  $4$  (●)  $\mu\text{M}$ .

which is typical of most small molecule protein kinase inhibitors (9, 20, 21). It was somewhat surprising that **4**, which is quite similar in structure and size to **1**, **2**, and **3**, clearly and consistently displayed an inhibition pattern that is competitive with both ATP and peptide (Figure 4). Replacing the 4'-phenoxy of **4** with an anilino group (**5**) maintained the competitiveness of **4** with both substrates (data not shown). Replacing the 6,7-dimethoxy of **4** with an amino at 7 (**6**) or eliminating both of the methoxy groups (**7**) did not perturb the inhibition pattern (data not shown) although such structural changes affected the binding affinity of the compounds for enzyme (see below).  $K_{is}$  and  $K_{ii}$  (Table 2), the slope and intercept inhibition constants, for these compounds were obtained by nonlinear least-squares fit of the inhibition data to eqs 2 or 3 according to the inhibition patterns established for these compounds. Subsequently,  $K_i$ , the inhibition constant for the binary complex EI (Table 2), was calculated by using eqs 4, 5, or 7 according to the mechanism of inhibition and which substrate was varied. The similarity in the  $K_i$  values obtained from varying ATP and peptide, as shown in Table 2, suggests internal consistency of the data. This result and the inhibition patterns determined for **1**–**7** indicate that the 4'-phenoxy in **4** and the 4'-anilino group in **5** are structural determinants for the change of the inhibition pattern from being only competitive with ATP, as displayed by **1**, **2**, and **3**, to becoming competitive with both ATP and peptide, as demonstrated for **4** and **5**.

From a structural standpoint, two possible mechanisms exist for an inhibitor to display competitiveness toward both substrates. In one scenario, an inhibitor physically occupies both binding sites and, thereby, prevents the binding of either substrate at their respective binding site. Such inhibitors are "physical" dual site inhibitors for which the displayed kinetic competitiveness against both substrates does not require structural changes in enzyme. Alternatively, an inhibitor

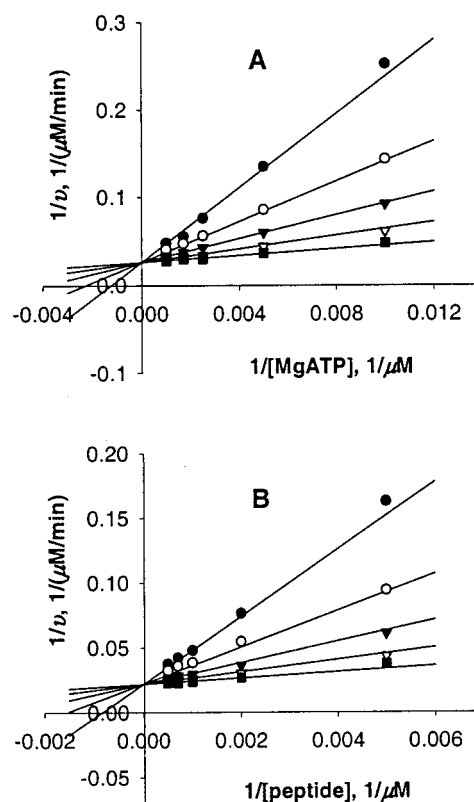


FIGURE 4: Inhibition of the dm-Src TK reaction by **4**. (A) Double-reciprocal plot of  $1/v$  vs  $1/[\text{MgATP}]$  ( $[\text{MgATP}] = 1000, 600, 400, 200$ , and  $100 \mu\text{M}$ ) at  $[I] = 0$  (■),  $0.04$  (▽),  $0.1$  (▼),  $0.2$  (○), and  $0.4$  (●)  $\mu\text{M}$ . (B) Double-reciprocal plot of  $1/v$  vs  $1/[\text{peptide}]$  ( $[\text{peptide}] = 2000, 1500, 1000, 500$ , and  $200 \mu\text{M}$ ) at  $[I] = 0$  (■),  $0.04$  (▽),  $0.1$  (▼),  $0.2$  (○), and  $0.4$  (●)  $\mu\text{M}$ .

Table 2: Pattern and Constants of Inhibition of dm-Src TK by Small Molecule Inhibitors at pH 7.5, 22 °C<sup>a</sup>

molecule	MI	variation of ATP		MI	variation of peptide				
		$K_{is}$	$K_i^b$		$K_{is}$	$K_{ii}$	$K_i^b$	$K_i'^c$	$\beta$
<b>1</b>	C	0.14	0.06	NC	0.29	1.20	0.13	0.32	2.5
<b>2</b>	C	0.18	0.20	NC	0.88	0.94	0.39	0.25	0.7
<b>3</b>	C	0.30	0.13	NC	0.53	2.06	0.23	0.55	2.4
<b>4</b>	C	0.040	0.015	C	0.036		0.016		
<b>5</b>	C	0.085	0.031	C	0.040		0.018		
<b>6</b>	C	1.67	0.62	C	1.44		0.64		
<b>7</b>	C	3.44	1.28	C	2.75		1.22		
<b>8</b>	C	6.27	2.32	C	7.41		3.29		
<b>9</b>	C	0.33	0.08	NC	0.46	6.14	0.21	1.65	8.1
<b>10</b>	C	0.84	0.62	NC	1.83	3.33	0.81	0.89	1.1

<sup>a</sup> All values are in micromolar. The slope and intercept inhibition constants,  $K_{is}$  and  $K_{ii}$ , respectively, were obtained from nonlinear least-squares analysis of data according to eqs 2 or 3 dependent upon the inhibition pattern the data represented. <sup>b</sup>  $K_i$ , the inhibition constant for the binary complex EI, was calculated by using eqs 4, 5, or 7, dependent upon the inhibition pattern, with  $[\text{ATP}] = 150 \mu\text{M}$  if peptide is the varied substrate or  $[\text{peptide}] = 500 \mu\text{M}$  if ATP is the varied substrate. <sup>c</sup>  $K_i'$ , the inhibition constant for the ternary complex EBI, was calculated by using eq 8, with  $[\text{ATP}] = 150 \mu\text{M}$ . The  $\beta$  values were calculated using eq 6; MI, mode of inhibition; C, competitive; NC, noncompetitive.

binds at one substrate-binding site of enzyme, and this binding induces a conformational change in the other site of the enzyme that excludes the binding of the other substrate. Such inhibitors are not physical dual site inhibitors and require structural changes in enzyme to show the kinetic competitiveness against both substrates. Whether 4-anilino-



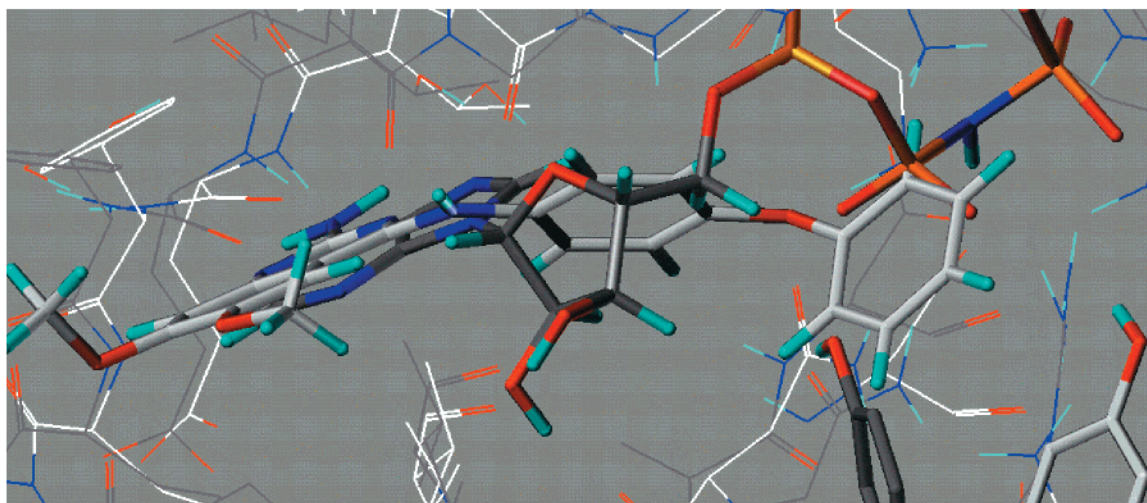
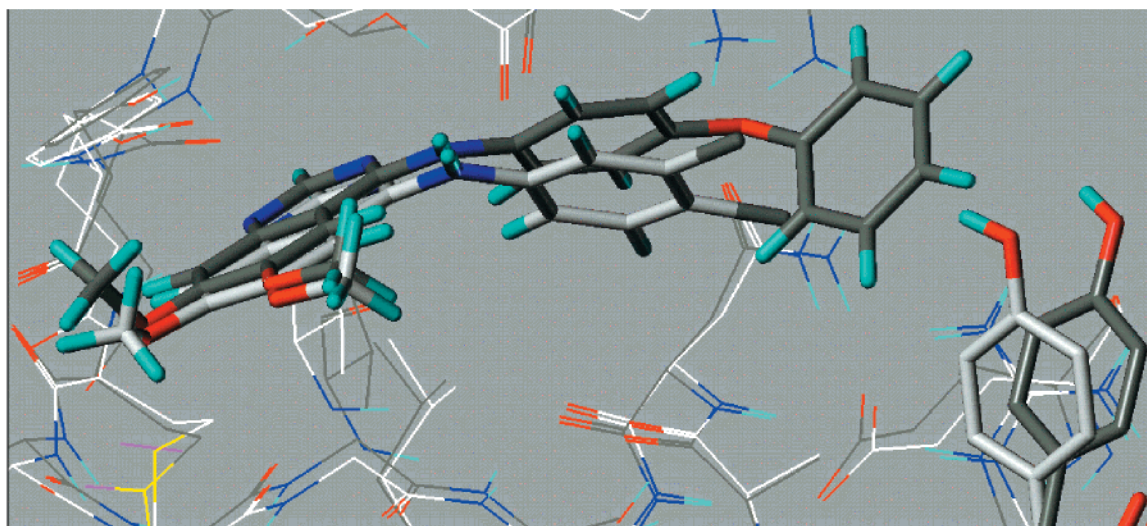
**A****B**

FIGURE 5: Computer-generated models of Src TK. (A) AMPPNP, **4**, and peptide substrate. Oxygen is red, phosphorus is orange, nitrogen is blue, carbon is either white or gray, hydrogen is aqua, and sulfur is yellow. The carbon atoms of AMPPNP are dark gray as is the substrate tyrosine group. The carbon atoms of the inhibitor **4** and the substrate in that model are pale gray. (B) Superimposed models of compounds **1** and **4** with the carbon atoms of **4** and the substrate tyrosine side chain in dark gray.

quinazolines **4–7** are physical dual site inhibitors cannot be unambiguously established solely from the kinetic experiments described above.

**Computer-Modeling of Src–Inhibitor Complexes.** Computer-modeling was performed to see if it is possible that those inhibitors that are kinetically competitive with both substrates may physically occupy part of the peptide-binding site and, thereby, prevent peptide binding in the ternary complex.

The crystal structure of Src TK bound with a nonhydrolyzable ATP analogue, AMPPNP, reported by Xu et al. (35) was used as a starting point. Into this structure was docked the peptide substrate used in the kinetic experiments with Src TK (acetyl-EEEEIYGEI-NH<sub>2</sub>). Initial starting points for this model were obtained by superposition of AMPPNP bound at the active site of Src with AMPPCP of the crystal structure (34) of IR TK, which is the only crystal structure available for protein tyrosine kinases where both an ATP analogue and a peptide substrate are bound simultaneously

at the active site. After the initial positions of the Src peptide substrate were obtained, structures of enzyme–inhibitor–peptide ternary complexes were obtained by docking inhibitors in conformations seen in CDK2 and p38 for similar compounds (24). The final structural models were obtained by conformational searches for the flexible bonds of the ligands first keeping protein and peptide rigid, followed by additional conformational searches allowing movement of the protein and peptide, with the found ligand conformations kept static. An alternative model for substrate binding has been presented in the work of Gaul et al. (36).

As shown in Figure 5A, the phenoxy group of **4** bound at the ATP site of Src collides with the tyrosyl of the peptide substrate if also bound to Src. The tyrosyl group will need to move by 5–6 Å in order to avoid such an atomic conflict. This movement is potentially highly energetic, resulting in loss of affinity of the peptide for the inhibitor-bound enzyme. Compared to the structure of Src with **4** binding at the ATP

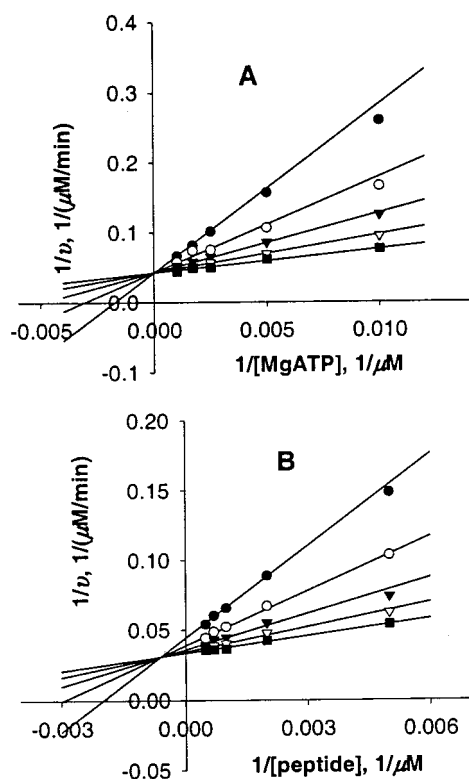


FIGURE 6: Inhibition of the dm-Src TK reaction by **9**. (A) Double-reciprocal plot of  $1/v$  vs  $1/[\text{MgATP}]$  ( $[\text{MgATP}] = 1000, 600, 400, 200, \text{ and } 100 \mu\text{M}$ ) at  $[\text{I}] = 0$  (■), 1 (▽), 3 (▼), 6.67 (○), and 10 (●)  $\mu\text{M}$ . (B) Double-reciprocal plot of  $1/v$  vs  $1/[\text{peptide}]$  ( $[\text{peptide}] = 2000, 1500, 1000, 500, \text{ and } 200 \mu\text{M}$ ) at  $[\text{I}] = 0$  (■), 1 (▽), 3 (▼), 6.67 (○), and 10 (●)  $\mu\text{M}$ .

site, **1** binds easily at the ATP site with the peptide substrate binding at the peptide site (Figure 5B). No distortion of the peptide is necessary. These data are consistent with the kinetic results where **4** is competitive with both ATP and

peptide and **1** is competitive with ATP and noncompetitive with peptide and suggest that these "dual site" inhibitors bearing a large 4'-substituent do compete physically with peptide substrate.

**Alternative Binding Modes of 9?** It was curious that the kinetic inhibition pattern displayed by **9**, which has a bulky 4'-substituent, was competitive with ATP but not with peptide (Figure 6), an exception to the dual site inhibition pattern displayed by other compounds having a bulky 4'-group. However, the affinity of the compound for Src TK determined from the noncompetitive binding mode was much higher ( $\sim 8$ -fold, the  $\beta$  value in Table 2) than the value determined from the competitive inhibition pattern, suggesting that the binding modes of **9** between its competitive and noncompetitive inhibitions may be different. Computer-modeling indicated that **9** can bind snugly at the ATP site of Src TK in the absence of peptide, but the 4'-group of **9** can fold back during binding in the presence of peptide that would make enough room for peptide binding (Figure 7), albeit that this binding mode is more energetic and, therefore, the binding less tighter.

**Potency and Selectivity of Dual Site Inhibitors.** Having identified the structural determinants for 4-anilinoquinazolines as dual site inhibitors of Src, we asked the question whether such dual site inhibitors would provide an advantage in potency and selectivity over the nondual site inhibitors. The  $\text{IC}_{50}$  values for inhibition of the nonreceptor tyrosine kinases Src and Lck and the two receptor tyrosine kinases VEGFR2 and C-fms were obtained for **4**, a dual site inhibitor, and **11**, a nondual site inhibitor. As shown in Table 3, there is a good correlation between the  $\text{IC}_{50}$  values for Src and Lck, which is not unexpected given the close homology between the two kinases. However, the dual site inhibitor **4** is more potent than the nondual site inhibitor **11** by a factor of 129 for Src and 28 for Lck. Both **11** and **4** are about

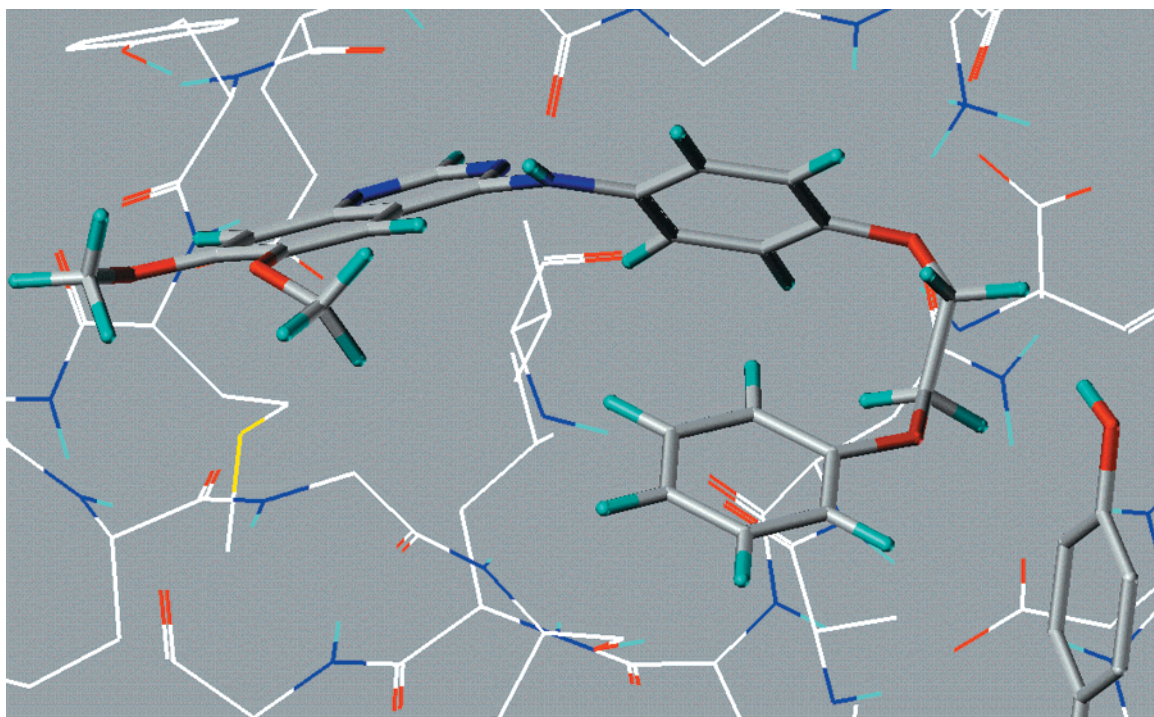
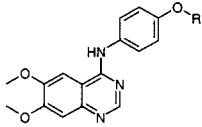
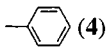


FIGURE 7: Computer-generated models of Src TK with **9** and peptide substrate. Oxygen is red, nitrogen is blue, carbon is either white or grey, hydrogen is aqua, and sulfur is yellow. The carbon atoms of the inhibitor **9** and the substrate tyrosine group are pale grey.



Table 3: Summary of IC<sub>50</sub> Values of **4** and **11** for the Inhibition of Src, Lck, ErbB2, VEGFR2, and C-fms and Selectivity Values of **4** vs **11** for Src over Lck, VEGFR2, and C-fms

-R	IC <sub>50</sub> , $\mu$ M (Selectivity)			
	Src	Lck	VEGFR2	C-fms
 <b>11</b>	5.6	2.5	0.46	20
 <b>4</b>	0.044 (1)	0.088 (5)	0.32 (88)	30 (190)

equally potent against VEGFR2 and C-fms. It is interesting that the nondual site inhibitor **11** is about equally potent in the inhibition of Src and C-fms whereas the dual site inhibitor **4** is much less potent in the inhibition of C-fms when compared to Src. To quantitate the selectivity of **4** and **11**, eq 9 was used:

$$\text{selectivity} = \left( \frac{\text{IC}_{50(2)}}{\text{IC}_{50(2r)}} \right) / \left( \frac{\text{IC}_{50(1)}}{\text{IC}_{50(1r)}} \right) \quad (9)$$

where IC<sub>50(1)</sub> and IC<sub>50(2)</sub> are, respectively, the values of **4** for enzymes 1 and 2 and IC<sub>50(1r)</sub> and IC<sub>50(2r)</sub> are, respectively, the values of **11** for enzymes 1 and 2. Thus, by having an anilino-phenoxy, **4** gains a selectivity of 5, 88, and 190 for Src over Lck, VEGFR2, and C-fms, respectively. This selectivity pattern was generally conserved for other dual site inhibitors (data not shown).

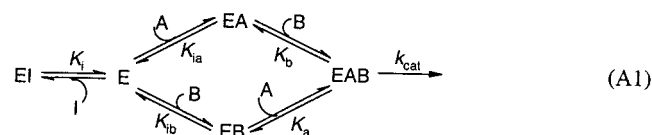
**Conclusion.** 4-Anilinoquinazolines with a bulky group at the 4'-position of the anilino group were shown to be kinetically competitive with both ATP and peptide. Such a "dual site" inhibition pattern may have resulted from a possible physical collision between the 4'-group and the phospho-accepting tyrosyl of peptide bound at the peptide-binding site of Src TK, as suggested from computer modeling. The dual site inhibitors appeared to have both enhanced potency and selectivity for Src TK. Future work to further explore such dual site inhibition may help design inhibitors with better potency and selectivity.

## ACKNOWLEDGMENT

Dr. Edgar Wood, Mr. Brad O'McDonald, and Ms. Wendy Liu are sincerely acknowledged for sharing unpublished inhibition data on VEGFR2 and C-fms.

## APPENDIX

A dual site inhibition mechanism is depicted as follows:



in which inhibitor I can only bind the free enzyme. Using the method outlined for derivation of equations for rapid

equilibrium mechanisms (31), the kinetic inhibition equation for the above dual site inhibition can be expressed as

$$v = \frac{VAB}{K_{ia}K_b \left( 1 + \frac{I}{K_i} \right) + K_aB + K_bA + AB} \quad (A2)$$

Rearranging eq A2 to express B as a fixed substrate and A as the varying substrate, we have

$$v = \frac{V_bA}{(K_a)_b \left( 1 + \frac{I}{K_i} \right) + A} \quad (A3)$$

in which

$$V_b = \frac{VB}{K_b + B} \quad (A4)$$

$$(K_a)_b = K_a \frac{K_{ib} + B}{K_b + B} \quad (A5)$$

and

$$K_{is} = K_i \left( 1 + \frac{B}{K_{ib}} \right) \quad (A6)$$

Solving eq A6 for K<sub>i</sub>, we have

$$K_i = \frac{K_{is}}{1 + \frac{B}{K_{ib}}} \quad (A7)$$

## REFERENCES

- Hunter, T. (1989) *Cell* 1, 1168–1181.
- Hunter, T. (1995) *Cell* 80, 225–236.
- Huang, P. S., and Heimbros, D. C. (1997) *Curr. Opin. Oncol.* 9, 94–100.
- Takeuchi, T., and Abe, T. (1998) *Int. Rev. Immunol.* 17, 365–381.
- Lewis, A. J., and Manning, A. M. (1999) *Curr. Opin. Chem. Biol.* 3, 489–494.
- Le Marchand-Brustel, Y. (1999) *Exp. Clin. Endocrinol. Diabetes* 107, 126–132.
- Fry, D. W., Kraker, A. J., Connors, R. C., Elliott, W. L., Nelson, J. M., Showalter, H. D., and Leopold, W. R. (1994) *Anticancer Drug Des.* 9, 331–351.

8. Lee, J. C., and Adams, J. L. (1995) *Curr. Opin. Biotechnol.* 6, 657–661.
9. Groundwater, P. M., Solomons, K. R. H., Drewe, J. A., and Munawar, M. A. (1996) *Prog. Med. Chem.* 33, 233–329.
10. Patrick, D. R., and Heimbroke, D. C. (1996) *Drug Discov. Today* 1, 325–330.
11. Traxler, P. M., Furet, P., Mett, H., Buchdunger, E., Meyer, T., and Lydon, N. (1997) *J. Pharm. Belg.* 52, 88–96.
12. Gray, N. S., Wodicka, L., Thunnissen, A.-M. W. H., Norman, T. C., Kwon, S., Espinoza, F. H., Morgan, D. O., Barnes, G., LeClerc, S., Meijer, L., Kim, S.-H., Lockhart, D. J., and Schultz, P. G. (1998) *Science* 281, 533–538.
13. Lawrence, D. S., and Niu, J. (1998) *Pharmacol. Ther.* 77, 81–114.
14. Bridges, A. J. (1999) *Curr. Med. Chem.* 6, 825–843.
15. Toledo, L. M., Lydon, N. B., and Elbaum (1999) *Curr. Med. Chem.* 6, 775–805.
16. Hanks, S. K. (1991) *Curr. Opin. Struct. Biol.* 1, 369–383.
17. Wei, L., Hubbard, S. R., Smith, R. F., and Ellis, L. (1994) *Curr. Opin. Struct. Biol.* 4, 450–455.
18. Denny, W. A., Rewcastle, G. W., Bridges, A. J., Fry, D. W., and Kraker, A. J. (1996) *Clin. Exp. Pharmacol. Physiol.* 23, 424–427.
19. Wakeling, A. E., Barker, A. J., Davies, D. H., Brown, D. S., Green, L. R., Cartledge, S. A., and Woodburn, J. R. (1996) *Breast Cancer Res. Treat.* 38, 67–73.
20. Traxler, P. M. (1997) *Expert Opin. Ther. Pat.* 7, 571–588.
21. Myers, M. R., He, W., and Hulme, C. (1997) *Curr. Pharm. Des.* 3, 473–502.
22. Ramdas, L., Obeysekere, N. U., Sun, G., McMurray, J. S., and Budde, R. J. A. (1999) *J. Pept. Res.* 53, 569–577.
23. Fry, D. W., Kraker, A. J., McMichael, A., Ambroso, L. A., Nelson, J. M., Leopold, W. R., Connors, R. W., and Bridges, A. J. (1994) *Science* 265, 1093–1095.
24. Shewchuk, L., Hassell, A., Wisely, B., Rocque, W., Holmes, W., Veal, J., and Kuyper, L. F. (2000) *J. Med. Chem.* 43, 133–138.
25. Bridges, A. J., Zhou, H., Cody, D. R., Rewcastle, G. W., McMichael, A., Showalter, H. D., Fry, D. W., Kraker, A. J., and Denny, W. A. (1996) *J. Med. Chem.* 39, 267–276.
26. Ellis, B., DeLacy, P., Weigl, D., Kassel, D., Patel, I., Wisely, G. B., Lewis, K., Overton, L., Kadwell, S., Kost, T., Hoffman, C., Barrett, G., Robbins, J., Knight, W. B., Edison, A., Huang, X., Berman, J., Rodriguez, M., and Luther, M. (1994) *J. Cell. Biochem.* 18 (Suppl. B), 276.
27. Barker, S. C., Kassel, D. B., Weigl, D., Huang, X., Luther, M. A., and Knight, W. B. (1995) *Biochemistry* 34, 4843–4851.
28. Edison, A. M., Barker, S. C., Kassel, D. B., Luther, M. A., and Knight, W. B. (1995) *J. Biol. Chem.* 270, 27112–27115.
29. Cleland, W. W. (1979) *Methods Enzymol.* 63, 103–138.
30. Boerner, R. J., Barker, S. C., and Knight, W. B. (1995) *Biochemistry* 34, 16419–16423.
31. Segel, I. H. (1975) *Enzyme Kinetics*, John Wiley and Sons, New York.
32. Berman, H. M., Westbrook, J., Feng, Z., Gilliland, G., Bhat, T. N., Weissig, H., Shindyalov, I. N., and Bourne, P. E. (2000) *Nucleic Acids Res.* 28, 235–242.
33. Mohamadi, F., Richards, N. G. J., Guida, W. C., Liskamp, R., Lipton, M., Caufield, C., Chang, G., Hendrickson, T., and Still, W. C. (1990) *J. Comput. Chem.* 11, 440–467.
34. Hubbard, S. R. (1997) *EMBO J.* 16, 5572–5581.
35. Xu, W., Doshi, A., Lei, M., Eck, M. J., and Harrison, S. C. (1999) *Mol. Cell* 3, 629–638.
36. Gaul, B. S., Harrison, M. L., Geahlen, R. L., Burton, R. A., and Post, C. B. (2000) *J. Biol. Chem.* 275, 16174–16182.

BI0100586